Desalination and Water Treatment
www.deswater.com
doi: 10.1080/19443994.2016.1178603

57 (2016) 29044–29057
December

Taylor & Francis
Taylor & Francis Group

The synergistic effect of organic foulants and their fouling behavior on the nanofiltration separation to multivalent ions

Fang Gao[a,b], Yuxing Sheng[a,*], Hongbin Cao[a,*], Yuping Li[a], Chunlei Su[a,b,c], Xiaoli Cui[d]

[a]*Key Laboratory of Green Process and Engineering, Institute of Process Engineering, Chinese Academy of Sciences, Beijing 100190, China, Tel./Fax: +86 10 82544844; emails: 232230204@qq.com (F. Gao), yxsheng@home.ipe.ac.cn (Y. Sheng), Tel./Fax: +86 10 82544839; email: hbcao@home.ipe.ac.cn (H. Cao), Tel./Fax: +86 10 82544844; emails: stringsplay@126.com (Y. Li), 564355246@qq.com (C. Su)*
[b]*University of Chinese Academy of Sciences, Beijing 100049, China*
[c]*School of Chemical Engineering, University of Xiangtan, Xiangtan 411105, China*
[d]*Jinzhou Titanium Industry Company, Ltd., Jinzhou 121005, China, Tel. +86 10 18940600335; Fax: +86 10 82544844; email: cuixiaolijzty@163.com*

Received 14 November 2015; Accepted 8 April 2016

ABSTRACT

This work aimed to determine the effect of organic foulants and fouling behavior on separation of multi-ions for nanofiltration (NF) membrane. Three model organic foulants (bovine serum albumin, lysozyme, and humic acid) were selected and studied in depth. The rejections of mono- and di-anions by virgin membrane varied with different organic foulants because of foulant-enhanced co-ion competition. Subsequent multi-ions separations by fouled membranes were different due to the zeta potential and structure of the fouling cake. In contrast to the single protein system, Cl^- and SO_4^{2-} rejection was reduced by HA fouled membrane. However, with added proteins in the HA solution, mixed systems experienced decreasing Cl^- rejection and increasing SO_4^{2-} rejection. In addition, solution chemistry (solution pH, ionic strength, and Ca^{2+}) had marked effect on the cake layer composition, likely due to the changing interaction between foulant and foulant, as well as between foulant and NF membrane. The suitable foulant cake structure could result enhanced in multi-ions separation. The synergistic mechanisms of organic foulants and cake were analyzed by calculated cake hydraulic resistance and zeta potential of fouled membranes.

Keywords: Nanofiltration; Multivalent anions separation; Organic foulant; Zeta potential; Cake-enhanced concentration polarization

1. Introduction

The application of membrane filtration to separate inorganic salt and reject natural organic matter (NOM) has gained momentum in recent years [1–3]. Given the relatively high permeate flux, low operation pressure and agents, application fields of nanofiltration (NF) process have become broader. In the field of separation of multivalent and monovalent ions, NF can be especially considered as an advantageous technique. The inherence of NF membrane contains a thin effective separation layer which has functionally active porous and surface electric charge [4,5]. Nevertheless, many obstructions controlling NF membrane performance in

*Corresponding authors.

ion separation and water recovery, especially due to ineluctable membrane fouling, are observed.

In previous years, studies on NF membrane used for the fractionation and separation of complex salts focused on its dominant effects and mechanisms, including (a) solution and electrolyte chemistry effect: anion separation reduced as pH decreased, due to co-ion competition and dominant-ion [6,7]. In addition to solute, the concentration and ion constitution can also affect the separation of multivalent ions [8,9]. (b) Membrane properties: knowledge of the effective membrane thickness, charge density, pore size, and hydrophilicity can affect the separation of mixed electrolytes [10–13]. (c) Finally, mechanisms for anion separation: a steric and Donnan exclusion was observed [14,15]. In practice, NF multi-salt separation plagued by residual organic substances in the feed was not mentioned. Previous studies on NF fouling behavior and mechanisms by residual organic substances focused on assessment criteria that permeate flux reduction by fouled membrane [16,17]. For example, Zhao et al. [18] performed bovine serum albumin (BSA) and humic acid (HA) fouling experiments with NF membrane. Flux measurements revealed severer fouling in combined fouling experiments than in individual experiments.

Relatively, only a few studies reported the effect of organic foulants and their fouling behavior on salt separation. For example, Luo et al. compared the rejection of NaCl by NF membrane in the absence or presence of HA, and found that the rejection of NaCl was enhanced by addition of HA because of strong electrostatic interaction [19,20]. Moreover, Bargeman et al. [21] indicated that slightly negative NaCl retentions were obtained due to the presence of glucose in the tight membranes. However, Li et al. [22] found that the addition of amino acid reduced the rejection of NH_4Cl, but subsequently enhanced rejection of $(NH_4)_2SO_4$. On fouling behavior influence, Mahlangu et al. [23] investigated the fouling behavior using sodium alginate and latex. NaCl rejections by fouled membrane at both single and mixed foulants were lower than that by clean membrane. However, Wang and Tang [24] found that the formation of fouling cake by combined alginate and lysozyme (LYS) reduced salt rejection. Relatively, the fouling cake by single foulant enhanced salt rejection. In terms of variant organic matters with different charges, co-ion competition between di- and mono-anions was more complicated in the presence of organic substances. Membrane properties could also be varied by fouling gel/cake on the membrane surface. The synergistic effect of both charged organic macromolecules and organic cake on the separation of complex salts was more complex and poorly understood. Therefore, an investigation into the synergistic mechanism of multi-ion separation at organic fouling systems is necessary.

The objectives of the current study were to investigate the effect of single and mixed organic foulants and their fouling behavior on separation of mono- and divalent ions by NF membrane. Three single (BSA, LYS, and HA) and two mixed organic substances (BSA + HA and LYS + HA) were used to model single and mixed fouling systems, respectively. By contradistinguishing different zeta potentials of organic foulants, and analyzing the zeta potential of membrane and fouling cake hydraulic resistance at variant ion strength, solution pH, and cation composition, the study may provide significant insights synergistic mechanisms of macromolecules and their fouling behavior on multi-ions separation.

2. Materials and methods

2.1. Model organic foulants

Humic substances and proteins have been identified as the major foulants in the effluent. Humic acid (HA, Sigma–Aldrich 53680), Bovine serum albumin (BSA, Sigma–Aldrich A1933, ≥98% purity), and lysozyme (LYS, Sigma–Aldrich L6876, ≥90% purity) were used as model foulants. A single foulant system (HA, BSA and LYS alone), and mixed foulant systems with dissolving equal amounts of BSA+ or LYS + HA were used to investigate the influence of organic substances and their fouling behavior on separation of polyvalent ions. Unless specified otherwise, all reagents and chemicals were of analytical grade. Ultrapure water (Milli Q, resistivity of 18.2 MΩ) was used to prepare working solutions.

2.2. Membrane filtration test

NF experiments were carried out in a laboratory scale cross-flow membrane filtration system consisting of a rectangular membrane module. The membrane area was 19.6 cm^2. A high antifouling thin-film composite membrane was used as NF membrane (NF GL by GE Osmonics, Inc. USA). A gear pump (WT3000–1JB–A, Longer Pump, China) adjusting the flow was used to transport feed solution. Applied pressure was adjusted with a needle valve and monitored using pressure transmitters (SSI Technologies, Inc. 0–25 bar, China). Permeate flux was measured using an electronic balance (Ohaus Instruments Co., Ltd. China) and recorded using a computer data logging system. During the filtration, the permeation and retention were recycled back to the feed tank at stated periods.

For each filtration test, a fresh membrane was immersed in ultrapure water until it was loaded into the test cell. The membrane was first compacted by pure water for 5 h to ensure the stable permeate flux. The duration of each test was about 30 h until the desired permeate flux reduction was obtained. Chloride and sulfate ion concentration in the initial and final permeates over 30 h fouling test, as well as the corresponding feed, was measured by ion chromatography (Dionex–550, USA). Every condition was measured at least two replicates. During the entire experiments, variant foulant systems (total organic foulant concentration of 20 mg L^{-1}, single foulant: 20 mg L^{-1} BSA, LYS and HA; mixed foulant: 10 mg L^{-1} BSA(or LYS) and 10 mg L^{-1} HA), feed pH (adjusted by the addition of 1 M HCl and NaOH solution), anionic strength range of 4–100 mM (molar concentration of NaCl and Na_2SO_4 was 2, 20 and 50 mM, respectively), and cation composition (Na^+ system: cations in the feed were only Na^+ ions; Na^+/Ca^{2+} system: cation in the feed were binary of Na^+ and Ca^{2+} ions; Ca^{2+} system: cation in the feed were only Ca^{2+} ions) were investigated. Unless specified otherwise, the following conditions were applied: applied pressure at 70 psi and temperature at 293 K in the entire experiments.

2.3. Theory

First, for the each fouling experiment, ultrapure water was filtrated through the membrane for 5 h to achieve stable permeate flux at the experimental conditions. In accordance with the stable permeate flux, the membrane hydraulic resistance was determined by:

$$R_m = \frac{\Delta P}{\mu J_w} \tag{1}$$

where R_m is the membrane hydraulic resistance, ΔP is the applied pressure, μ is the dynamic viscosity of pure water at experimental temperature, and J_w is the pure water permeate flux. The feed solution combined with amount of dissolved inorganic salt, the driving force permeation is the difference between the applied pressure. Thus, the permeate flux can be described by:

$$J = \frac{\Delta P - \Delta \pi_m}{\mu R_m} \tag{2}$$

where J_w is the permeate flux, and $\Delta \pi_m$ is the transmembrane osmotic pressure. When the permeate flux is in steady-state condition, the permeate can be related to the membrane, bulk and permeate salt concentrations. In accordance with film theory fitted for NF separation, it derived the following equation [25]:

$$\Delta \pi_m = f_{os}(c_m - c_p) = f_{os} c_b r_0 \exp\left(\frac{J}{k_0}\right) \tag{3}$$

where c_m is the molar salt concentration on the membrane surface, c_p is the molar salt concentration in the permeate, c_b is the molar salt concentration in the bulk, r_0 is the salt rejection, k_0 is the mass-transfer coefficient. f_{os} is osmotic coefficient that converted the molar salt concentration to an osmotic pressure ($f_{os} = 3\,RT$ in this experiment, R is the universal gas constant and T is the absolute temperature).

As discussed previously, a synergistic effect of dissolve NOMs and inorganic salts in the feed was observed. Hence, we can derive the existing of a capital model to describe the fouling behavior and selective rejection of ions of the experimental membrane, composed of organic fouling cake and cake-enhanced concentration polarization. The membrane permeate flux can be described by the resistance in series model [26], as follows:

$$J = \frac{\Delta P - \Delta \pi_m^*}{\mu(R_m + R_c)} \tag{4}$$

where J is the permeate flux at any experimental time, $\Delta \pi_m^*$ is the transient osmotic pressure drop, and R_c is the transient hydraulic resistance of the organic fouling cake layer. Transient osmotic pressure drop was determined by the following equation:

$$\Delta \pi_m^* = f_{os} c_b r_i \exp\left(\frac{J}{k}\right) \tag{5}$$

where r_i is the intrinsic membrane salt rejection, and k is the fouling mass-transfer coefficient. During the fouling experiment, the thickness of the organic cake layer affected both the diffusion and convection of salt ions in and around the cake layer. The intrinsic membrane salt rejection, r_i is described as Eq. (7):

$$r_i = \frac{c_m - c_p}{c_m} \tag{6}$$

$$\ln\left(\frac{1-r}{r}\right) = \ln\left(\frac{1-r_i}{r_i}\right) + \frac{J}{k} \tag{7}$$

The decline in flux showed the effect of solute mass-transfer on the cake layer thickness. Thus, fouling mass-transfer coefficient k combined with thick deposit layer may be described by [27,28]:

$$k = 1.468\left(\frac{QD_{\infty}^{2}}{W(H-\delta_c)^2 L}\right)^{1/3} \quad (8)$$

where D_∞ is the bulk diffusion coefficient of the solute, Q is the volumetric feed flow rate, W is the channel width, H is the channel height, and L is the channel length. Considering the increase in transient osmotic pressure drop with the formation of deposited cake layer and aggravated fouling behavior, the cake transient hydraulic resistance was described by Eq. (9), as follows:

$$R_c = \frac{1}{\mu J}\left(\Delta P - f_{os} c_b r_i \exp\left(\frac{J}{k}\right)\right) - R_m \quad (9)$$

Anion rejection, r, is calculated using Eq. (8), where c_p and c_f are ion concentrations in the permeate and the feed, respectively.

$$r(\%) = \frac{c_f - c_p}{c_f} \times 100 \quad (10)$$

Separation between Cl^- and SO_4^{2-}, S, which can be simply expressed in terms of rejection at the corresponding ion, is defined by Eq. (11):

$$S = \frac{c_{Cl^-,p}}{c_{Cl^-,f}} \times \frac{c_{SO_4^{2-},f}}{c_{SO_4^{2-},p}} = \frac{100 - r_{Cl^-}}{100 - r_{SO_4^{2-}}} \quad (11)$$

S_0 is defined as separation of multi-ion by virgin membrane at the initial stage of the test. S_{30} is the separation of multi-ions by fouled membrane at the final stage of the test. S_t is the corresponding separation increment over 30 h.

3. Results and discussion

3.1. Zeta potential of single and mixed foulants

Zeta potential values of single and mixed foulants in the feed solution were measured by a Zetasize Nano–ZS (Beckman Coulter, Inc., USA), respectively. The zeta potential values are presented in Table 1. For both mixed foulant systems, the zeta potential values declined with the increase in solution pH.

Table 1
Zeta potential of single and mixed foulants

	Zeta potential of single foulants (mV)				Zeta potential of mixed foulants (mV)	
pH	BSA	LYS	HA	pH	BSA + HA	LYS + HA
6.5	−6.9	11.3	−27.2	4.5	−10.8	14.2
				6.5	−21.5	0.2
				8.5	−25.2	−20.3
				10.5	−26.7	−20.5

3.2. Single vs. mixed fouling systems

Fig. 1 shows the permeate flux behavior of NF membrane in the presence of single and mixed foulants. For the single fouling system, flux reductions over 30 h of fouling test were 17.2, 11.4, and 8.8%, respectively, at corresponding BSA, LYS, and HA alone. The results showed that the larger size of organic foulant in the feed adsorbed more easily on the membrane surface [29–31]. By contrast, flux reduction caused by binary mixed foulants of BSA/LYS and HA was much severer than those at either BSA or LYS alone. This condition was attributed to the HA adsorption of aggregations to the protein surface, and to the hindered back diffusion of polyvalent salts [32]. Moreover, the flux reduction of LYS + HA was more severe than that of BSA + HA, due to the electrostatic interaction of aggregate protein–HA. At pH 6.5, the zeta potential of aggregate BSA − HA was −21.5 mV.

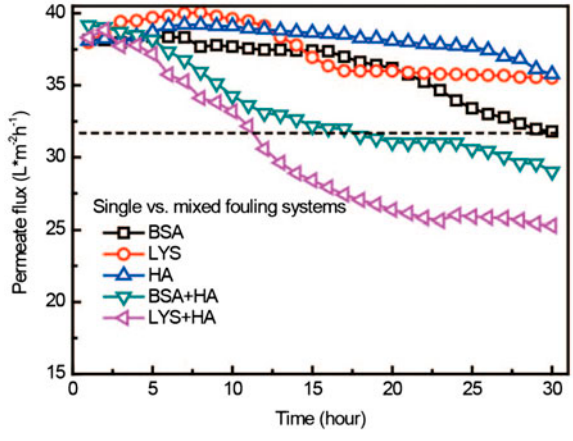

Fig. 1. Comparison of the fouling behavior by single and mixed systems, test conditions: single foulant 20 mg L^{-1} (BSA, LYS, and HA alone); mixed foulants 10 mg L^{-1} HA and 10 mg L^{-1} BSA (LYS), molar concentration ratio of Cl^-: SO_4^{2-} 1:1, at Na^+ system, pH 6.5, and temperature at 293 K.

However, monomer LYS − HA was near zero potential, which promoted destabilized LYS − HA aggregating and forming the larger size polymer [33]. The electrostatic repulsion between the homo-charged BSA − HA and membrane also retarded the fouling behavior, similarly compared with that by uncharged LYS − HA [34].

The effect of single and mixed types of foulant, and their fouling behavior on the rejection of polyvalent ions were investigated. Fig. 2 depicts that rejection between chloride and sulfate ions by virgin membrane was significant. Furthermore, the results indicated that NF can separate available polyvalent and monovalent ions. At the initial filtration stage, either single foulant or mixed foulants can play a significant role on separation of multi-ions due to their electric interaction and co-ion competition [22]. Organic substance also had positive charge. More Cl^- ions combined with LYS molecules permeated through the NF membrane, even the rejection of Cl^- by virgin membrane at LYS was −9.2% and lower than those at other fouling systems. In comparison with BSA and HA alone, an electrostatic repulsive force between negatively charged molecules and anions retarded Cl^- and SO_4^{2-} permeation to the membrane surface [35]. Moreover, for mixed systems, this repulsion amplified by a large size of BSA(LYS) − HA may play a stronger role in increasing the rejection of anions. Fig. 2 also shows the changing rejection of both ions that occurred with fouling behavior under variant fouling systems. For single protein, the rejection of Cl^- and SO_4^{2-} increased

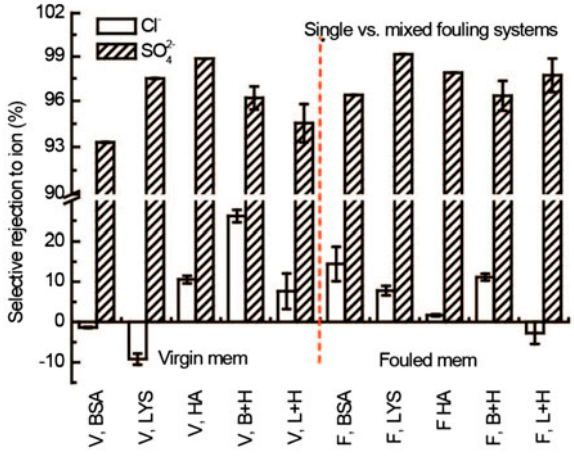

Fig. 2. Comparison of the rejection to multi-ion by single and mixed systems, test conditions: single foulant 20 mg L^{-1} (BSA, LYS, and HA alone); mixed foulants 10 mg L^{-1} HA and 10 mg L^{-1} BSA (LYS), molar concentration ratio of Cl^-: SO_4^{2-} 1:1, at Na^+ system, pH 6.5, and temperature at 293 K.

with aggravating fouling behavior, due to the cake structure and membrane pore constriction and block. When feed contained only protein, the formation of a disulfide bond between protein molecules may be considered hindrance to ion permeation in the cake layer. Conversely, fouling system was added with a relatively small size of charged organic solute such as HA, the rejection of Cl^- declined over 30 h of fouling test, due to the cake loose structure [36]. Although HA molecules were considered a bridge between proteins, which wrapped around the protein molecule, they may break the disulfide bond, and subsequently, form a tortuous pathway for the back transport of anions. This cake by protein–HA hindered inorganic salt inside the organic gel back diffusion, and thus enhanced ion concentration on the membrane [28]. With regard to the rejection of SO_4^{2-} in both single and mixed systems, all the rejections during the fouling experiment remained stable over time, illustrating either co-ion competition by organic solute or the influence of the cake structure were negligible.

3.3. Effect of pH on flux behavior and multi-ion rejection

Considering that the zeta potential of both foulants and NF membrane contributed significantly to the fouling behavior and separation of multi-ions, and varied with changing pH, the effect of solution pH on mixed fouling system fouling behavior was investigated. Fig. 3 shows ~35% flux loss of both systems observed at pH 4.5. At pH 6.5, the flux reductions were 26% (BSA + HA) and 34% (LYS + HA), respectively. These results may be accounted for by the −33.9 mV zeta potential value of BSA − HA aggregate, which was much stronger than the zero potential of LYS − HA aggregate. Electrostatic repulsion between foulant and membrane can delay membrane fouling [37–39]. With increasing solution pH, the flux reductions of both systems alleviated to only 8% at pH 10.5. This result suggests that HA among protein molecules may play an electric screening effect, similar to the phenomenon at high concentration salt [24]. In the current work, both BSA and LYS carried strong negative charges on themselves at alkaline conditions, Electrostatic repulsion between proteins and homo-charged HA played a dominant role.

Considering that the rejection of multi-ion changed due to different pH values and the corresponding fouling, the lowest initial rejection to Cl^- and SO_4^{2-} at pH 4.5 was observed, as shown in Fig. 4. Moreover, the rejection of Cl^- was negative, and the values were –11.9% (BSA + HA) and –4.1% (LYS + HA), respectively. This result was attributed to the rapid and

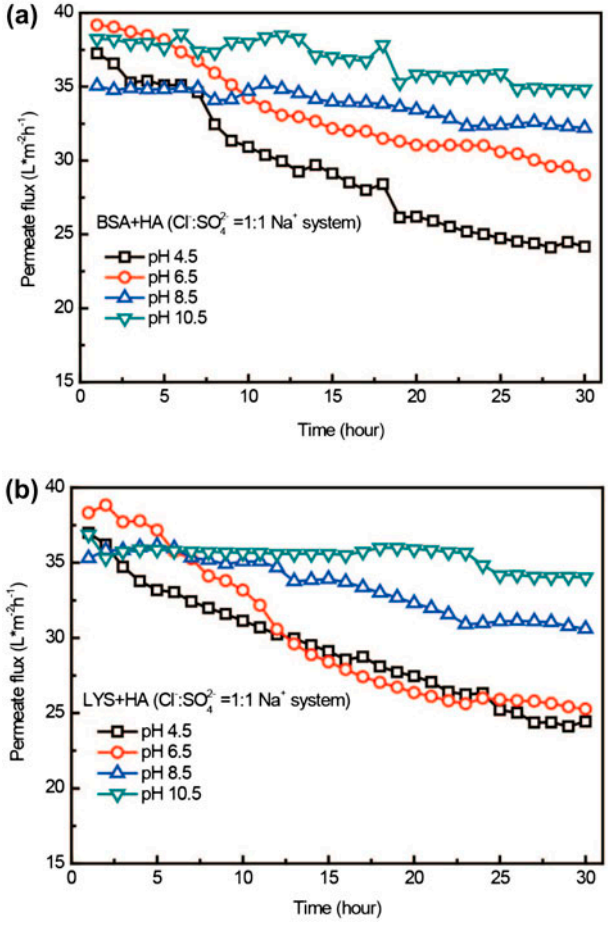

Fig. 3. Effect of pH on mixed system fouling behavior, (a) BSA + HA; (b) LYS + HA. Test conditions: total organic foulant containing 10 mg L^{-1} HA and 10 mg L^{-1} BSA, molar concentration ratio of Cl^-: SO_4^{2-} 1:1, at Na^+ system, ionic strength of 4 mM, and temperature at 293 K.

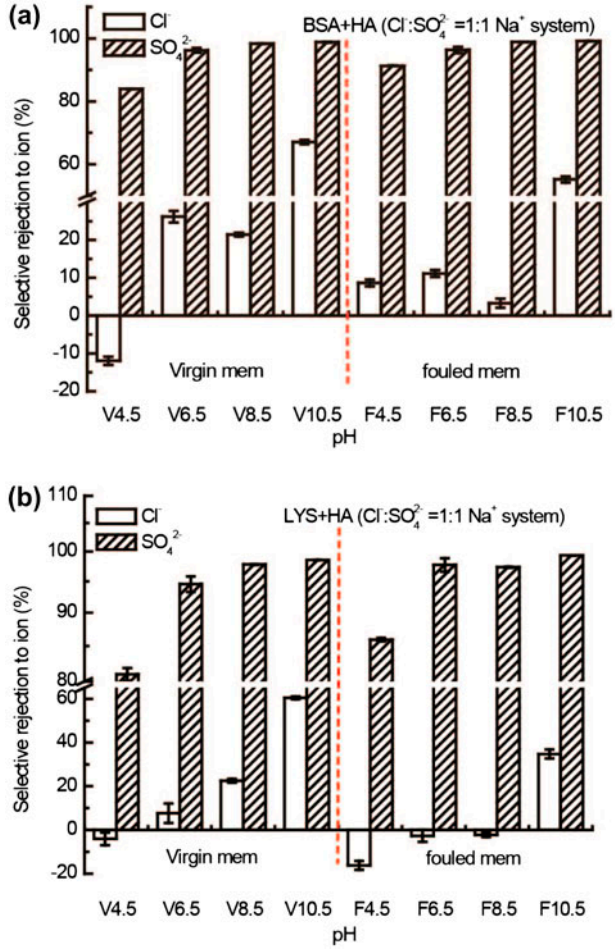

Fig. 4. Effect of fouling behavior on the selective rejection of multivalent ions at different pH values, (a) BSA + HA system; (b) LYS + HA system. P.S. V 4.5/(6.5, 8.5, and 10.5): V represents the virgin membrane at the corresponding pH value; F 4.5/(6.5, 8.5, and 10.5): F represents the fouled membrane over 30 h test.

easier osmosis of H^+ ions into the NF membrane compared with other cations. Zeta potential of the NF membrane surface likewise weakened with lower pH [40]. Hence, the large amount of Cl^- and SO_4^{2-} ions in the feed migrated into the permeate strata because of influences of the Donnan equilibrium and weak electrostatic repulsion. As shown in Fig. 6(a) and (b), the initial rejection of Cl^- and SO_4^{2-} at both systems increased with increasing pH, which was due to the strengthening of both co-ion competition and electrostatic repulsion between anions and membrane [41]. As the amount of strong electrolyte OH^- in the feed increased, competition between anions (Cl^- and SO_4^{2-}) and OH^- resulted in the increasing rejection of Cl^- and SO_4^{2-}. Moreover, within the pH range above the isoelectric point of the membrane, the negative charge of the membrane enhanced with increasing pH. Thus, the electrostatic repulsive force between Cl^- and SO_4^{2-} and membrane also improved the ion rejection. During the fouling test, for both systems, in most cases, a decreasing rejection of Cl^- and a stable rejection of SO_4^{2-} were observed in Fig. 4. The results were consistent with those under variant ionic strength, due to enhancing concentration polarization by fouling cake. However, for BSA + HA systems, the rejection of Cl^- by fouled membrane was higher than that by virgin membrane at pH 4.5, which was consistent with the results in the rejection of multi-ion for a single BSA system. The results were attributed to the main molecule structures at BSA + HA, which were BSA − HA − BSA by disulfide bond among BSA molecules.

3.4. Effect of ionic strength on flux behavior and multi-ion rejection

As mentioned above, the effect of mixed foulants representing real effluent conditions on flux behavior and multi-ion separation under variant conditions was worth of investigating. Fig. 5 shows the effect of ionic strength on initial permeate flux and fouling behavior at both BSA + HA and LYS + HA systems. The initial permeate flux declined from 39.2 to 14.3 L m^{-2} h^{-1} at BSA + HA, and from 38.3 to 12.2 L m^{-2} h^{-1} at LYS + HA, respectively, when the ionic strength ($Cl^- + SO_4^{2-}$) increased from 4 to 100 mM in the feed. This result was attributed to the increase in osmosis pressure, which enhanced ionic strength in the feed at a constant operation pressure according to Eqs. (2) and (3). After 30 h fouling tests, the permeate flux at both fouling systems declined by ~30% at an ionic strength of 4 and 40 mM, due to the formation of the organic cake in the membrane. At ion strength of 100 mM, the flux loss at LYS + HA was about 17%, and was less with only 10% at BSA + HA. Increasing ionic strength suppressed interactions between protein and HA, and thus impeded macro-molecular polymer formation. The reason applying for the phenomenon was that the isolation layer between protein and HA, and between organic foulants and membrane surface by electrostatic screening [33,42].

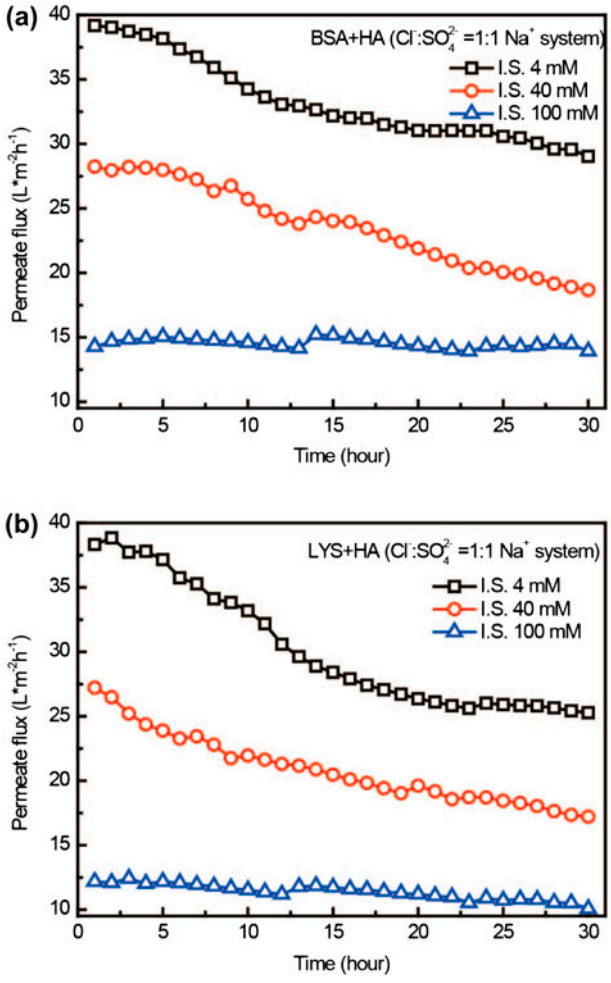

Fig. 5. Effect of ionic strength on mixed system fouling behavior, (a) BSA + HA system; (b) LYS + HA system. Test conditions: total organic foulant containing 10 mg L^{-1} HA and 10 mg L^{-1} BSA (LYS), molar concentration ratio of Cl^-: SO_4^{2-} is 1:1, at Na^+ system, pH 6.5, and temperature at 293 K.

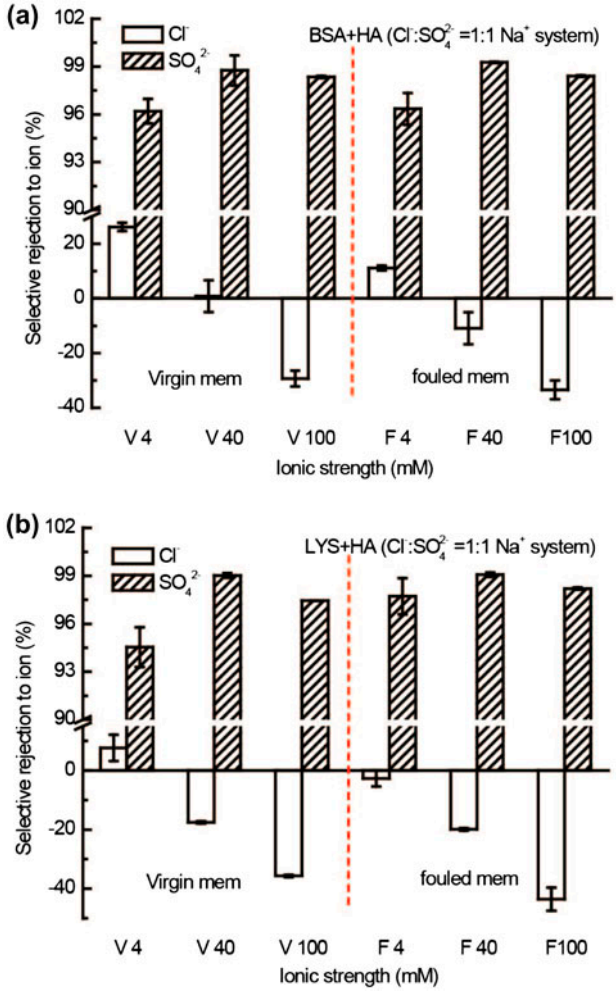

Fig. 6. Effect of fouling behavior on selective rejection of multivalent ions at variant ionic strength, (a) BSA + HA system; (b) LYS + HA system. P.S. V 4/(40 and 100): V represents the virgin membrane at corresponding ionic strength; F 4/(40 and 100): F represents the fouled membrane over 30 h test.

Fig. 6 shows that the effect of ionic strength on Cl^- and SO_4^{2-} rejections by virgin membrane at both BSA + HA and LYS + HA systems. The initial Cl^- rejection declined with an increasing amount of ion concentration. However, the initial SO_4^{2-} rejection was influenced slightly by ionic strength, which was explained by the Donnan effect and ions competition contributed to negative rejection of monovalent ion at near neutral pH [41]. As the experiment proceeded, parts (a) and (b) of Fig. 6 also present that the change in fouling degree contributed to the rejection of multi-ion. Decrease in Cl^- rejection and stable SO_4^{2-} rejection also occurred in both systems. In BSA + HA system, Cl^- rejection with at ion strength of 4, 40, or 100 mM reduced to 11.3, −10.9, or and −33.4% over 30 h, respectively. SO_4^{2-} rejection remained statically above 95%, which was attributed to the weakening charge of membrane surface and concentration polarization [15,35]. The fouling cake was formed by BSA − HA adsorbed on the membrane surface, and tortuous channels within cake layer may hinder the back diffusion of ions. A weakening electrostatic repulsive force between fouled membrane and anions also led to more ions deposited on the membrane surface. In comparison, Fig. 6(b) presents the initial Cl^- and SO_4^{2-} rejections, and their rejections over 30 h fouling test at LYS + HA. The results indicated that Cl^- rejection by both virgin and fouled membrane under three types of ionic strength was lower that at corresponding BSA + HA, due to the increase in weakening charge and reinforced concentration polarization. Both rejections were attributed to unstable LYS − HA polymers with zero potential at pH 6.5.

3.5. Effect of cation composition on flux behavior and multi-ion rejection

Given the different integrations of multivalent cation and variant types of foulants, the experiments investigated the effect of different cation compositions on the both systems fouling behavior at the same experimental conditions were conducted. As Fig. 7 depicted, when cations in the feed were replaced by Ca^{2+} partly or totally, the initial permeate flux at either BSA + HA or LYS + HA declined to some extent, due to much easier rejection of Ca^{2+} by the NF membrane, leading to enhanced osmotic pressure. For BSA+HA, part (a) of Fig. 7 also illustrates that the flux reduction increased first then decreased with the increase in added Ca^{2+} ions. Moreover, the most severe losses observed at Na^+/Ca^{2+} system. At this pH, aggregation between BSA and HA was contributed mainly by functional interaction. The effect of

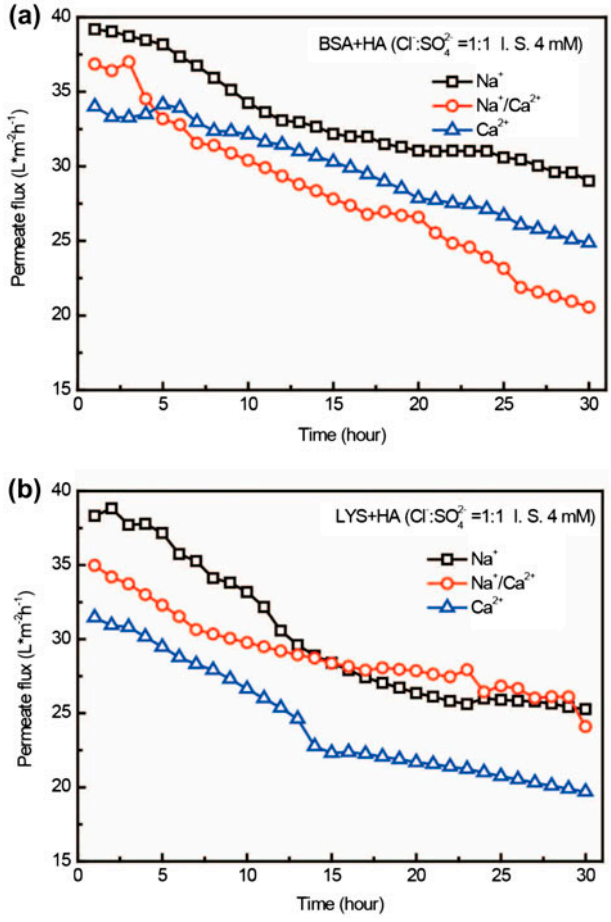

Fig. 7. Effect of cation composition on mixed system fouling behavior, (a) BSA + HA; (b) LYS + HA. Test conditions: total organic foulant containing 10 mg L^{-1} HA and 10 mg L^{-1} BSA, molar concentration ratio of Cl^-: SO_4^{2-} is 1:1, at pH 6.5, ionic strength of 4 mM, and temperature at 293 K.

combined Na^+ and Ca^{2+} ions on aggravating BSA + HA fouling can also be explained as follows: low concentration of Na^+ ions weaken the electrostatic force of organic aggregates BSA − HA, moreover Ca^{2+} ions bridges between aggregates, and promotes foulants adsorbed on the membrane surface [43,44]. However, for LYS + HA system, the Ca^{2+} influence was not obvious in part (b) of Fig. 7. The results can be due to the competition of polymers (formed by the oppositely charged LYS and HA molecules), and added with Ca^{2+} ions with positively charged LYS for carboxyl negatively charged sites in HA [24,45].

The results of the comparative study on the effect of cation composition and fouling behavior on the rejection of mono-and di-ions indicate that rejection of Cl^- by virgin membrane, for both systems, increased. Moreover, effect of cation composition on rejection of

SO_4^{2-} was almost ignored with the increasing proportion of Ca^{2+} in Fig. 8. The reason for the changing of anion rejection was dominated by divalent cations, caused by both electrostatic screening and Donnan effect [9,46]. On the contrary, compared with increasing rejection of Cl^- at BSA + HA, the growing rate at LYS + HA was larger, which may be due to occurrence of Ca^{2+}–carboxyl in HA molecules at LYS + HA. Relatively, Ca^{2+}–carboxyl occurred at both BSA and HA molecules at BSA + HA. Therefore, more free Ca^{2+} ions can impede more anions migrating to the permeate. During fouling experiment, rejection of Cl^- by fouled membrane over 30 h was reduced under three types of cation compositions at both systems, due to the fouling cake formed by polymers. Rejections of SO_4^{2-} by BSA (or LYS) + HA fouled membranes remained above 90% within variant Na^+/Ca^{2+} molar proportions of 1:0, 0.5:0.5, and 0:1, as shown in Fig. 8(a) and (b).

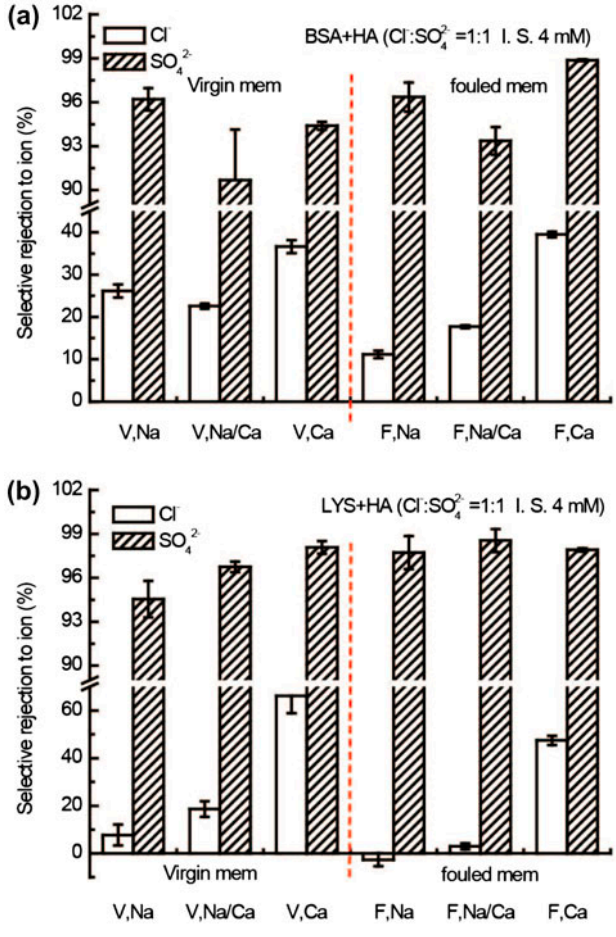

Fig. 8. Effect of fouling behavior on selective rejection of multivalent ions at variant cation compositions, (a) BSA + HA system; (b) LYS + HA system. P.S. V Na/(Na/Ca and Ca): V represents the virgin membrane at corresponding cation composition; F Na/(Na/Ca and Ca): F represents the fouled membrane over 30 h test.

3.6. Characterization of fouled NF membrane

The morphologies of the fouled NF membranes in the tests were measured by SEM. As shown in parts (a)–(d) of Fig. 9, a considerable difference between the fouled membranes under variant fouling systems, and fouling cake layers and their thicknesses at both systems at pH 6.5 was observed. The formation of fouling cake on the membrane surfaces also altered the interfacial properties of the membrane and influenced the permeate flux and rejections of Cl^- and SO_4^{2-}. Table 2 also depicts the thicknesses of cakes at both systems under variant conditions. The values were consistent with permeate flux reductions according to Figs. 3, 5, and 7.

Zeta potential values of virgin and fouled membranes under variant conditions were depicted in Table 3. For the virgin NF membrane, its zeta potential was more susceptible to solution pH, and the value decreased with increasing pH. Zeta potential measured by different salts was slightly different according to Teixeira et al. [12]. Table 3 shows the zeta potential values of fouled membranes at both mixed foulants under variant conditions. Changing potential was attributed to different foulants with charge deposited on the membrane. Although the foulant had similar charges under different conditions, such as, at LYS + HA, the potential value of the fouled membrane with an ionic strength of 100 mM was stronger than that with ionic strengths of 4 and 40 mM. This result was attributed to the amount of foulant adsorbed on the membrane surface, which was so little that negatively charged sites of membrane surface remitted by organic foulants were limited. The results are consistent with the above rejection of Cl^- and SO_4^{2-}.

3.7. Synergetic mechanism of foulants and fouling behavior on multi-ion separation

3.7.1. Effect of pH

Both solution pH and membrane fouling degree can influence the separation degree of Cl^- and SO_4^{2-}. Table 4 shows the separation of Cl^- and SO_4^{2-} by virgin membrane at both systems, enhanced with higher pH due to co-ion competition caused by pH disproportion in feed and permeate. Moreover, the increasing rate at BSA + HA was higher than that at LYS + HA, due to co-ion competition enhanced by charged organic foulants. Considering the zeta

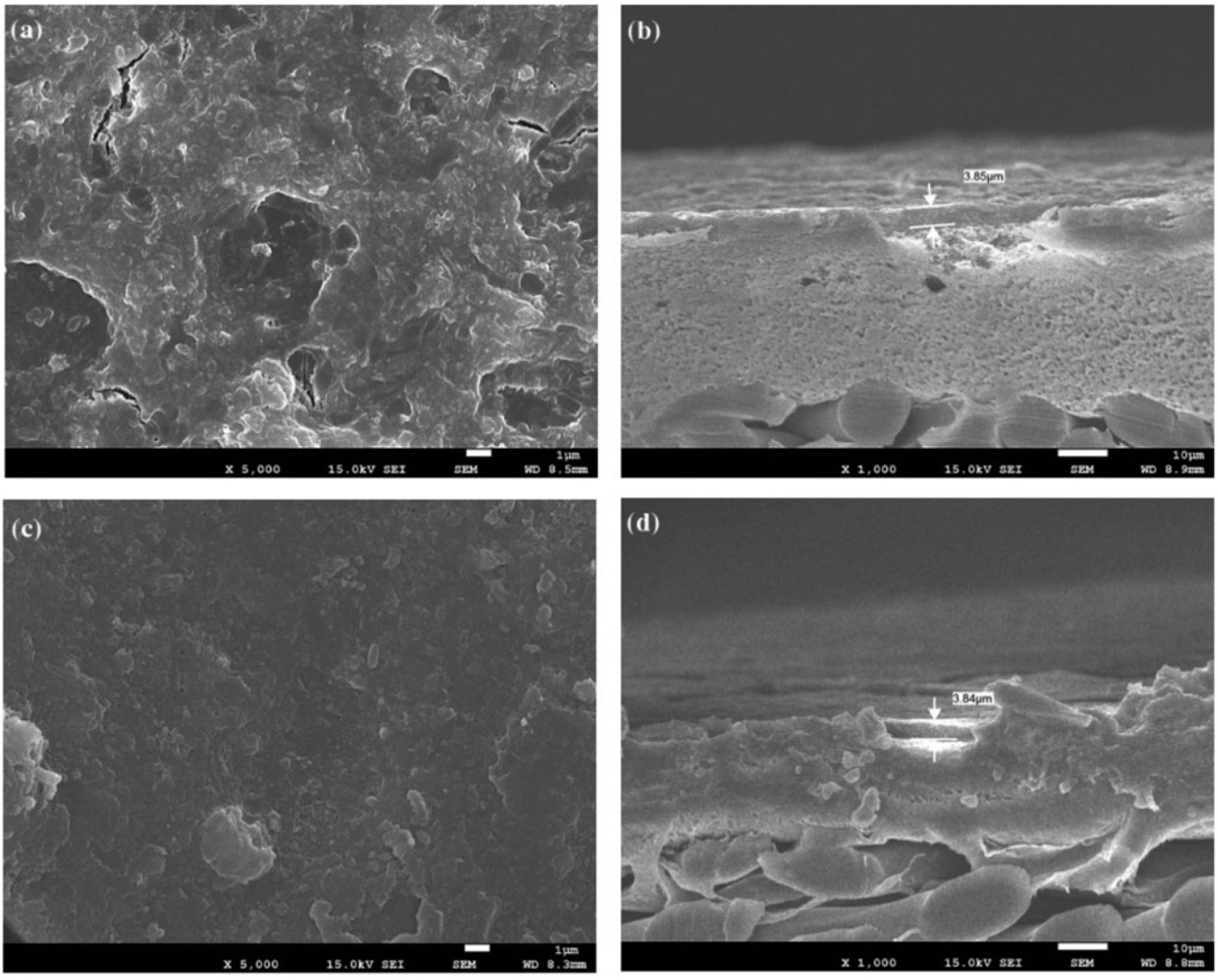

Fig. 9. SEM images of fouled membrane: (a and b) BSA + HA system; (c and d) LYS+HA system. Test conditions: ionic strength of 4 mM, molar concentration ratio of Cl^-: SO_4^{2-} is 1:1, cation: Na^+, pH 6.5.

Table 2
The thicknesses of fouling cake layers at both systems under variant conditions

	pH				Ionic strength (mM)			Cation composition		
Cake (μm)	4.5	6.5	8.5	10.5	4	40	100	Na^+	Na^+/Ca^{2+}	Ca^{2+}
BSA + HA	2.81	2.53	1.78	1.41	2.53	3.85	1.50	2.53	4.07	3.48
LYS + HA	4.07	3.84	2.83	1.59	3.84	3.84	1.78	3.84	4.03	4.60

potential of BSA − HA was lower than that of LYS − HA at a corresponding pH value, more negatively charged foulants played stronger competitiveness for multi-ion separation [20,47]. However, separation reduced as pH increased to 10.5. Electrostatic forces between similarly charged proteins (BSA and LYS) and HA hinder aggregation between BSA (LYS) and HA, thus weakening polymer-enhanced co-ion competition. Besides, electric repulsion between anions and membrane surface strengthened and impeded anion migration. A comparison of the separation of Cl^- and SO_4^{2-} by fouled membrane between

Table 3
Zeta potential of virgin and fouled membranes at both systems under variant conditions

	pH				Ionic strength (mM)			Cation composition		
Zeta (mV)	4.5	6.5	8.5	10.5	4	40	100	Na^+	Na^+/Ca^{2+}	Ca^{2+}
Virgin mem	−42.1	−51.6	−55.6	−58.3	−51.6	−50.2	−42.7	−51.6	−52.4	−50.7
Fouled mem										
BSA + HA	−12.2	−29.2	−33.6	−41.3	−29.2	−23.3	−30.3	−29.2	−20.4	−19.6
LYS + HA	−9.2	−15.1	−21.4	−27.6	−15.1	−15.5	−23.5	−15.1	−13.2	−11.8

Table 4
Separation of Cl^- and SO_4^{2-} by virgin and fouled membranes at variant pH

	BSA + HA				LYS + HA			
	S_0	S_{30}	S_t	$R_c \times 10^{13}$ (m^{-1})	S_0	S_{30}	S_t	$R_c \times 10^{13}$ (m^{-1})
pH 4.5	7	11	4	2.4	6	8	2	2.3
pH 6.5	22	34	12	1.5	18	34	16	2.2
pH 8.5	39	80	41	0.4	26	51	25	0.7
pH 10.5	16	45	29	0.4	20	66	44	0.4

both systems, results indicated that the fouling cake on the membrane contributed to an increasing separation of multi-ion as shown in Table 4. Within the pH range of 4.5–6.5, the contribution of cake for separation was lower than that within the pH range of 8.5–10.5. Obstruction of ion migration was enhanced by foulant cake, which was attributed to the thicker and tighter thickness of cake layer at lower pH, compared with that at alkaline condition. By contrast, cake resistance (R_c) at variant systems and conditions was similar. However, the increasing degree of separation of multi-ion was different, such as S_t (LYS + HA pH 10.5) > S_t (BSA + HA pH 8.5) > S_t (BSA + HA pH 10.5). These results were consistent with zeta potential values of fouled membrane as Table 3 shown. Which was attributed to the weakening electrostatic repulsion between anions and cake by mixed foulants [28,48]. At a pH range of 8.5–10.5, the zeta potential of both mixed foulants was negative. The electric repulsive force between homo-charged anions and fouled membrane was weaker, with a weakening charge of fouled membrane.

3.7.2. Effect of ionic strength

For both fouling systems, the separation of Cl^- and SO_4^{2-} enhanced with increasing ionic strength, which was attributed to the promotion of co-ion competition, and enlargement of membrane pore size due to high ionic strength [49]. Therefore, Cl^- ions with small size and low charge permeated more easily through the membrane. Increasing separation at BSA + HA was also slightly higher than that at LYS + HA, due to co-ion competition enhanced by charged organic foulant. Table 5 also illustrated that the foulant cake can partly contribute to the separation of Cl^- and SO_4^{2-} at both systems, due to Donnan and dielectric exclusion effects [8,12], and concentration polarization enhanced by the fouling cake [27]. Furthermore, the results also indicated that effect of increasing degree of separation on separation of multi-ions at LYS + HA was more than at BSA + HA in Table 5. The reason can be summarized as follows: (1) formation of the thicker organic gel by LYS − HA may hinder more ion diffusion; and (2) zeta potential of fouled membrane surface with LYS − HA cake was weaker than that with BSA − HA cake as shown in Table 3. Thus, the repulsion between anions and fouled membrane at BSA+HA was stronger than that between anions and fouled membrane at LYS + HA, since the zeta potential of LYS − HA polymer was close to the zero potential, compared with BSA − HA at pH 6.5

3.7.3. Effect of calcium ions

The separation behavior of Cl^- and SO_4^{2-} by virgin and fouled membranes at variant cation compositions was studied. Table 6 shows a decreasing separation by virgin membrane occurred with the increase of added Ca^{2+} ions at BSA + HA. The influence of Ca^{2+} at

Table 5
Separation of Cl^- and SO_4^{2-} by virgin and fouled membranes at variant ionic strength

	BSA + HA				LYS + HA			
	S_0	S_{30}	S_t	$R_c \times 10^{13}$ (m^{-1})	S_0	S_{30}	S_t	$R_c \times 10^{13}$ (m^{-1})
4 mM	22	34	12	1.5	18	34	16	2.2
40 mM	50	110	60	2.2	59	120	61	2.5
100 mM	64	65	1	0.3	54	72	18	0.9

Table 6
Separation of Cl^- and SO_4^{2-} by virgin and fouled membranes at variant cation composition

	BSA + HA				LYS + HA			
	S_0	S_{30}	S_t	$R_c \times 10^{13}$ (m^{-1})	S_0	S_{30}	S_t	$R_c \times 10^{13}$ (m^{-1})
Na	22	34	12	1.5	18	34	16	2.2
Na/Ca	8	12	4	3.4	20	48	28	2.0
Ca	10	30	20	1.6	17	26	9	2.6

LYS + HA was not significant. The phenomenon may be attributed to different charges and structures of BSA and LYS molecules [50–52]. At BSA + HA system, carboxyl groups in negatively charged BSA and HA molecules chelated with Ca^{2+}. This activity reduced the negative charge of BSA − HA aggregate, which remitted competition between anions and negatively charged organic foulants. However, for LYS + HA system, the charge between LYS and HA was opposite and the interaction between them was electrostatic attraction. With added Ca^{2+} in the feed, Ca^{2+} also competed with LYS for the negatively charged sites in HA, leading to positively charged LYS molecules released to the feed. The migration of charged LYS molecules to membrane surface may offset the influence of Ca^{2+} on increasing rejection of anions by Donnan effect. Simultaneously, Table 6 also reveals that the formation of cake layer on membrane surface at either BSA + HA and LYS + HA system, when feed contained Ca^{2+} ions, was beneficial in enhancing the separation of multi-ions. However, the result that the growing rate of separation decreased with aggravating fouling behavior contradicted that at Na^+ system alone under variant ionic strength. The reason may be due to the tighter structure of cake by Ca^{2+} bridging effect. Apart from the interaction between proteins and HA molecules by Ca^{2+} ions, Ca^{2+} can bridge between aggregates, i.e. BSA − HA (LYS − HA), and reduce the interfacial energy between aggregates, as well as between aggregates and membrane [24,53]. Thus, the incompressible fouling cake is formed. Not only did the cake hinder ion diffusion, but it also prevented anion permeation.

4. Conclusion

The fouling behavior and selective rejection of multi-ion by NF at single and mixed organic fouling systems were investigated. All experimental results represented were synergistic effects of model organic foulants as well as those fouling behavior on separation of multi-ion. Single foulant influenced NF selective rejection of Cl^- and SO_4^{2-} ions due to charged macromolecule competition. For the single protein system, rejection of Cl^- ions increased with aggravating fouling behavior. However, when feed contained HA molecules, the rejection of Cl^- ions reduced due to varying fouling cake structures. When foulants were complex in the feed, the influence of charged macromolecules and their fouling cakes on NF membrane separation behavior to Cl^- and SO_4^{2-} ions was enhanced further. For both mixed fouling systems, increasing pH can alleviate fouling behavior, relatively, which is disadvantageous of separation of multi-ion. Moreover, compared with acidic condition, the formation of cake contributed more to improving multi-salt separation at alkaline condition. With increasing ionic strength, the fouling behavior declined. Inversely, the separation degree of Cl^- and SO_4^{2-} ions increased. In comparison with BSA + HA system, separation degree at LYS + HA system was more significant with aggravating fouling behavior, due to cake-enhanced concentration polarization. When cations in the feed were replaced by part or total calcium ions, different permeate flux reductions were observed at both mixed systems. The separation of multi-ion also decreased by steric hindrance and electrostatic effect. The results of the investigation on

the effect of organic cake in combined with Ca^{2+} on multi-ion separation indicated that the most increasing separation degree did not occur with the severest fouling behavior. This finding suggested that incompressible metal complex cake can impede anion diffusion, as well as hinder Cl^- and SO_4^{2-} ion permeation.

Nomenclature

c_m	—	molar salt concentration on the membrane surface (mol m^{-3})
c_p	—	molar salt concentration in the permeate (mol m^{-3})
c_b	—	molar salt concentration in the bulk (mol m^{-3})
D_∞	—	bulk diffusion coefficient of the solute (m^2 s^{-1})
f_{os}	—	osmotic coefficient (Pa m^3 mol^{-1})
H	—	channel height (m)
J	—	permeate flux (m^3 m^2 s^{-1})
J_w	—	pure water permeate flux (m^3 m^2 s^{-1})
k_0	—	mass-transfer coefficient (m^3 m^2 s^{-1})
k	—	fouling mass-transfer coefficient (m^3 m^2 s^{-1})
L	—	channel length (m)
ΔP	—	applied pressure (Pa)
Q	—	volumetric feed flow rate (m^3 s^{-1})
R_m	—	membrane hydraulic resistance (m^{-1})
R_c	—	hydraulic resistance of organic fouling cake layer (m^{-1})
r_0	—	salt rejection (%)
r	—	rejection of anion (%)
r_i	—	intrinsic membrane salt rejection (%)
S	—	separation between Cl^- and SO_4^{2-} (dimensionless)
W	—	channel width (m)
μ	—	solution dynamic viscosity (Pa s)
$\Delta\pi_m$	—	osmotic pressure (Pa)
$\Delta\pi_m^*$	—	fouling osmotic pressure (Pa)

References

[1] D. Johnson, F. Galiano, S.A. Deowan, J. Hoinkis, A. Figoli, N. Hilal, Adhesion forces between humic acid functionalized colloidal probes and polymer membranes to assess fouling potential, J. Membr. Sci. 484 (2015) 35–46.

[2] V. Yangali-Quintanilla, A. Sadmani, M. McConville, M. Kennedy, G. Amy, Rejection of pharmaceutically active compounds and endocrine disrupting compounds by clean and fouled nanofiltration membranes, Water Res. 43 (2009) 2349–2362.

[3] B. Van der Bruggen, Integrated membrane separation processes for recycling of valuable wastewater streams: Nanofiltration, membrane distillation, and membrane crystallizers revisited, Ind. Eng. Chem. Res. 52 (2013) 10335–10341.

[4] A. Yaroshchuk, M.L. Bruening, E.E.L. Bernal, Solution-Diffusion–Electro-Migration model and its uses for analysis of nanofiltration, pressure-retarded osmosis and forward osmosis in multi-ionic solutions, J. Membr. Sci. 447 (2013) 463–476.

[5] D.L. Oatley, L. Llenas, R. Pérez, P.M. Williams, X. Martínez-Lladó, M. Rovira, Review of the dielectric properties of nanofiltration membranes and verification of the single oriented layer approximation, Adv. Colloid Interface Sci. 173 (2012) 1–11.

[6] J.-J. Qin, M.H. Oo, H. Lee, B. Coniglio, Effect of feed pH on permeate pH and ion rejection under acidic conditions in NF process, J. Membr. Sci. 232 (2004) 153–159.

[7] S. Szoke, G. Patzay, L. Weiser, Characteristics of thin-film nanofiltration membranes at various pH-values, Desalination 151 (2003) 123–129.

[8] C. Labbez, P. Fievet, A. Szymczyk, A. Vidonne, A. Foissy, J. Pagetti, Analysis of the salt retention of a titania membrane using the "DSPM" model: Effect of pH, salt concentration and nature, J. Membr. Sci. 208 (2002) 315–329.

[9] J. Tanninen, M. Mänttäri, M. Nyström, Effect of salt mixture concentration on fractionation with NF membranes, J. Membr. Sci. 283 (2006) 57–64.

[10] W.R. Bowen, H. Mukhtar, Characterisation and prediction of separation performance of nanofiltration membranes, J. Membr. Sci. 112 (1996) 263–274.

[11] W.R. Bowen, A.W. Mohammad, N. Hilal, Characterisation of nanofiltration membranes for predictive purposes—Use of salts, uncharged solutes and atomic force microscopy, J. Membr. Sci. 126 (1997) 91–105.

[12] M.R. Teixeira, M.J. Rosa, M. Nystrom, The role of membrane charge on nanofiltration performance, J. Membr. Sci. 265 (2005) 160–166.

[13] M. Mänttäri, A. Pihlajamäki, M. Nyström, Effect of pH on hydrophilicity and charge and their effect on the filtration efficiency of NF membranes at different pH, J. Membr. Sci. 280 (2006) 311–320.

[14] A. Szymczyk, C. Labbez, P. Fievet, A. Vidonne, A. Foissy, J. Pagetti, Contribution of convection, diffusion and migration to electrolyte transport through nanofiltration membranes, Adv. Colloid Interface Sci. 103 (2003) 77–94.

[15] A. Pérez-González, R. Ibáñez, P. Gómez, A.M. Urtiaga, I. Ortiz, J.A. Irabien, Nanofiltration separation of polyvalent and monovalent anions in desalination brines, J. Membr. Sci. 473 (2015) 16–27.

[16] D.T. Myat, M.B. Stewart, M. Mergen, O. Zhao, J.D. Orbell, S. Gray, Experimental and computational investigations of the interactions between model organic compounds and subsequent membrane fouling, Water Res. 48 (2014) 108–118.

[17] X.Q. Cheng, L. Shao, C.H. Lau, High flux polyethylene glycol based nanofiltration membranes for water environmental remediation, J. Membr. Sci. 476 (2015) 95–104.

[18] F. Zhao, K. Xu, H. Ren, L. Ding, J. Geng, Y. Zhang, Combined effects of organic matter and calcium on biofouling of nanofiltration membranes, J. Membr. Sci. 486 (2015) 177–188.

[19] V. Freger, T.C. Arnot, J.A. Howell, Separation of concentrated organic/inorganic salt mixtures by nanofiltration, J. Membr. Sci. 178 (2000) 185–193.

[20] J. Luo, S. Wei, Y. Su, X. Chen, Y. Wan, Desalination and recovery of iminodiacetic acid (IDA) from its sodium chloride mixtures by nanofiltration, J. Membr. Sci. 342 (2009) 35–41.

[21] G. Bargeman, J.B. Westerink, O.G. Miguez, M. Wessling, The effect of NaCl and glucose concentration on retentions for nanofiltration membranes processing concentrated solutions, Sep. Purif. Technol. 134 (2014) 46–57.
[22] S.-l. Li, C. Li, Y.-s. Liu, X.-l. Wang, Z.-a. Cao, Separation of l-glutamine from fermentation broth by nanofiltration, J. Membr. Sci. 222 (2003) 191–201.
[23] T.O. Mahlangu, E.M.V. Hoek, B.B. Mamba, A.R.D. Verliefde, Influence of organic, colloidal and combined fouling on NF rejection of NaCl and carbamazepine: Role of solute–foulant–membrane interactions and cake-enhanced concentration polarisation, J. Membr. Sci. 471 (2014) 35–46.
[24] Y.-N. Wang, C.Y. Tang, Nanofiltration membrane fouling by oppositely charged macromolecules: Investigation on flux behavior, foulant mass deposition, and solute rejection, Environ. Sci. Technol. 45 (2011) 8941–8947.
[25] E.M.V. Hoek, A.S. Kim, M. Elimelech, Influence of crossflow membrane filter geometry and shear rate on colloidal fouling in reverse osmosis and nanofiltration separations, Environ. Eng. Sci. 19 (2002) 357–372.
[26] A.S. Kim, A.N.L. Ng, Hydraulic permeability of polydispersed cake layers: An analytic approach, Desalination 207 (2007) 144–152.
[27] E.M.V. Hoek, M. Elimelech, Cake-enhanced concentration polarization: A new fouling mechanism for salt-rejecting membranes, Environ. Sci. Technol. 37 (2003) 5581–5588.
[28] A.E. Contreras, A. Kim, Q. Li, Combined fouling of nanofiltration membranes: Mechanisms and effect of organic matter, J. Membr. Sci. 327 (2009) 87–95.
[29] L. Palacio, C.C. Ho, P. Prádanos, A. Hernández, A.L. Zydney, Fouling with protein mixtures in microfiltration: BSA–lysozyme and BSA–pepsin, J. Membr. Sci. 222 (2003) 41–51.
[30] Y.-N. Wang, C.Y. Tang, Fouling of nanofiltration, reverse osmosis, and ultrafiltration membranes by protein mixtures: The role of inter-foulant-species interaction, Environ. Sci. Technol. 45 (2011) 6373–6379.
[31] N. Her, G. Amy, H.-R. Park, M. Song, Characterizing algogenic organic matter (AOM) and evaluating associated NF membrane fouling, Water Res. 38 (2004) 1427–1438.
[32] W.S. Ang, A. Tiraferri, K.L. Chen, M. Elimelech, Fouling and cleaning of RO membranes fouled by mixtures of organic foulants simulating wastewater effluent, J. Membr. Sci. 376 (2011) 196–206.
[33] Y.-N. Wang, C.Y. Tang, Protein fouling of nanofiltration, reverse osmosis, and ultrafiltration membranes—The role of hydrodynamic conditions, solution chemistry, and membrane properties, J. Membr. Sci. 376 (2011) 275–282.
[34] S.P. Palecek, A.L. Zydney, Intermolecular electrostatic interactions and their effect on flux and protein deposition during protein filtration, Biotechnol. Prog. 10 (1994) 207–213.
[35] S. Lee, J. Cho, M. Elimelech, Influence of colloidal fouling and feed water recovery on salt rejection of RO and NF membranes, Desalination 160 (2004) 1–12.
[36] Q. Li, M. Elimelech, Synergistic effects in combined fouling of a loose nanofiltration membrane by colloidal materials and natural organic matter, J. Membr. Sci. 278 (2006) 72–82.
[37] M. Elimelech, W.H. Chen, J.J. Waypa, Measuring the zeta (electrokinetic) potential of reverse osmosis membranes by a streaming potential analyzer, Desalination 95 (1994) 269–286.
[38] A.E. Childress, M. Elimelech, Effect of solution chemistry on the surface charge of polymeric reverse osmosis and nanofiltration membranes, J. Membr. Sci. 119 (1996) 253–268.
[39] R. Chan, V. Chen, The effects of electrolyte concentration and pH on protein aggregation and deposition: Critical flux and constant flux membrane filtration, J. Membr. Sci. 185 (2001) 177–192.
[40] S. Bandini, J. Drei, D. Vezzani, The role of pH and concentration on the ion rejection in polyamide nanofiltration membranes, J. Membr. Sci. 264 (2005) 65–74.
[41] J. Luo, Y. Wan, Effects of pH and salt on nanofiltration—A critical review, J. Membr. Sci. 438 (2013) 18–28.
[42] H. Mo, K.G. Tay, H.Y. Ng, Fouling of reverse osmosis membrane by protein (BSA): Effects of pH, calcium, magnesium, ionic strength and temperature, J. Membr. Sci. 315 (2008) 28–35.
[43] S. Hong, M. Elimelech, Chemical and physical aspects of natural organic matter (NOM) fouling of nanofiltration membranes, J. Membr. Sci. 132 (1997) 159–181.
[44] S. Lee, J. Cho, M. Elimelech, Combined influence of natural organic matter (NOM) and colloidal particles on nanofiltration membrane fouling, J. Membr. Sci. 262 (2005) 27–41.
[45] S.J. Li, Structural details at active site of hen egg white lysozyme with di- and trivalent metal ions, Biopolymers 81 (2006) 74–80.
[46] S. Bason, V. Freger, Phenomenological analysis of transport of mono- and divalent ions in nanofiltration, J. Membr. Sci. 360 (2010) 389–396.
[47] M. Nilsson, G. Trägårdh, K. Östergren, The influence of pH, salt and temperature on nanofiltration performance, J. Membr. Sci. 312 (2008) 97–106.
[48] L. Ouyang, R. Malaisamy, M.L. Bruening, Multilayer polyelectrolyte films as nanofiltration membranes for separating monovalent and divalent cations, J. Membr. Sci. 310 (2008) 76–84.
[49] M. Elimelech, X. Zhu, A.E. Childress, S. Hong, Role of membrane surface morphology in colloidal fouling of cellulose acetate and composite aromatic polyamide reverse osmosis membranes, J. Membr. Sci. 127 (1997) 101–109.
[50] P.J. Sadler, J.H. Viles, ^{1}H and ^{113}Cd NMR investigations of Cd^{2+} and Zn^{2+} binding sites on serum albumin: Competition with Ca^{2+}, Ni^{2+}, Cu^{2+}, and Zn^{2+}, Inorg. Chem. 35 (1996) 4490–4496.
[51] M. Lepoitevin, M. Jaber, R. Guégan, J.-M. Janot, P. Dejardin, F. Henn, S. Balme, BSA and lysozyme adsorption on homoionic montmorillonite: Influence of the interlayer cation, Appl. Clay Sci. 95 (2014) 396–402.
[52] S. Bi, B. Pang, T. Wang, T. Zhao, W. Yu, Investigation on the interactions of clenbuterol to bovine serum albumin and lysozyme by molecular fluorescence technique, Spectrochim. Acta, Part A 120 (2014) 456–461.
[53] C. Jarusutthirak, S. Mattaraj, R. Jiraratananon, Influence of inorganic scalants and natural organic matter on nanofiltration membrane fouling, J. Membr. Sci. 287 (2007) 138–145.